CHAPTER 3

RESULTS AND DISSCUSSION

In this chapter, crystal structures of three new nickel-polyoxovanadates of chemical formula $[V_{18}O_{42}X][Ni(C_2H_8N_2)_2]_3[Ni(H_2O)_4](NH_4)_3$ where X = Cl^- (Ni-POV-Cl) and Br^- (Ni-POV-Br) and $[V_{18}O_{42}X][Ni(C_2H_8N_2)_2]_3(NH_4)_3$ where X = I^- (Ni-POV-I), are described. The influences of halide anions on the crystal structures are discussed. Different approaches in determining the valence state of the involving vanadium atoms are present.

3.1 Structural description of Ni-POV-Cl and Ni-POV-Br

Single crystal X-ray analysis reveals the growth crystals to possess analogous structures of chemical formula $[V_{18}O_{42}X][Ni(C_2H_8N_2)_2]_3[Ni(H_2O)_4](NH_4)_3$ where X = Cl^- (Ni-POV-Cl) and Br- (Ni-POV-Br), and to crystallize in the same monoclinic *C2/c* (No. 15) space group. It is even more interesting to make a note on the cell parameters of Ni-POV-Cl and Ni-POV-Br that they are exactly the same; a = 12.7320(7)Å, b = 26.915(2)Å, c = 21.1968(13)Å, β = 92.783(5)°, V = 7255.2(8)Å^3 and Z = 4. The crystallographic data of these two compounds are summarized in Table 3.1, and will be described in the next few paragraphs. In solving and refining the crystal structures of Ni-POV-Cl and Ni-POV-Br, the direct method was applied, from which the

positions of all non-hydrogen atoms were located and assigned on the different Fourier maps. They were then refined by full-matrix least-squares analysis. All of the non-hydrogen atoms except O32 and N11 of Ni-POV-Cl were refined anisotropically. The hydrogen atoms of both structures were generated according to the attached atoms and refined using a riding model, except for those of the nitrogen atoms of NH_4^+cations which could not be located. Atomic coordinates and the isotropic or the equivalent isotropic displacement parameters for Ni-POV-Cl and Ni-POV-Br are listed in Table 3.2 and Table 3.3, respectively.

Figure 3.1 shows asymmetric units for the structure of Ni-POV-Cl and Ni-POV-Br, comprising of ten crystallographically unique V atoms and over forty O atoms. Each vanadium is coordinated to the terminal O_t atom which is located at the apex of a square pyramid, and the other four O_b atoms of the oxo-bridge V-(μ_3-O)-V at the basal positions. The notation of $[VO_5]_{sp}$ can therefore be correctly used in describing each vanadium of the structures. Eighteen of the $[VO_5]_{sp}$ units share their common edges *via* twenty four-μ_3-O atoms to form a $\{V_{18}O_{42}\}$ cluster with either Cl^- or Br^- anion encapsulated in the middle, which therefore result in the formation of $\{V_{18}O_{42}Cl\}$ and $\{V_{18}O_{42}Br\}$ clusters (Figure 3.2). The established $\{V_{18}O_{42}Cl\}$ and $\{V_{18}O_{42}Br\}$ clusters adopt the less symmetric pseudorhombicuboctahedral D_{4d} symmetry alike, which is expectedly preferable to the higher T_d symmetry when small anions like Cl^- or Br^- are to be encapsulated. This may be explained by the presence of only weak attraction between the cluster shell and the encapsulated anion [8].

Table 3.1 Crystallographic data and structural refinement parameters for Ni-POV-Cl and Ni-POV-Br.

	Ni-POV-Cl	**Ni-POV-Br**
Empirical formula	$[V_{18}O_{42}Cl][Ni(C_2H_8N_2)_2]_3$ $[Ni(H_2O)_4](NH_4)_3$	$[V_{18}O_{42}Br][Ni(C_2H_8N_2)_2]_3$ $[Ni(H_2O)_4](NH_4)_3$
Formula weight	2345.92	2390.37
Crystal description	Dark green bar	Dark green bar
Crystal size/mm^3	0.40 × 0.16 × 0.05	0.40 × 0.16 × 0.05
Crystal system	Monoclinic	Monoclinic
Space group	*C2/c*	*C2/c*
a/ Å	12.7320(7)	12.7320(7)
b/ Å	26.915(2)	26.915(2)
c/ Å	21.1968(13)	21.1968(13)
α/ °	90.000	90.000
β/ °	92.783(5)	92.783(5)
γ/ °	90.000	90.000
Unit cell volume/ Å^3	7255.2(8)	7255.2(8)
Z	4	4
ρ_{calc}/ g.cm^{-3}	2.14	2.18
T/ K	150(2)	150(2)
Radiation (λ/ Å)	MoKα(0.71073)	MoKα(0.71073)
μ/ mm^{-1}	3.34	3.85
θ_{min}, θ_{max}	2.8, 28.2	2.7, 34.8
Total data collected	18505	14095
Unique data	7765	14095
Parameters refined	434	457
Restrains no.	0	0
Goodness of fit	0.902	0.831
R, R_w (all data)	0.172, 0.242	0.124, 0.202
R, Rw (I>Xσ(I))	0.088, 0.208 (I>4σ(I))	0.067, 0.177 (I>4σ(I))

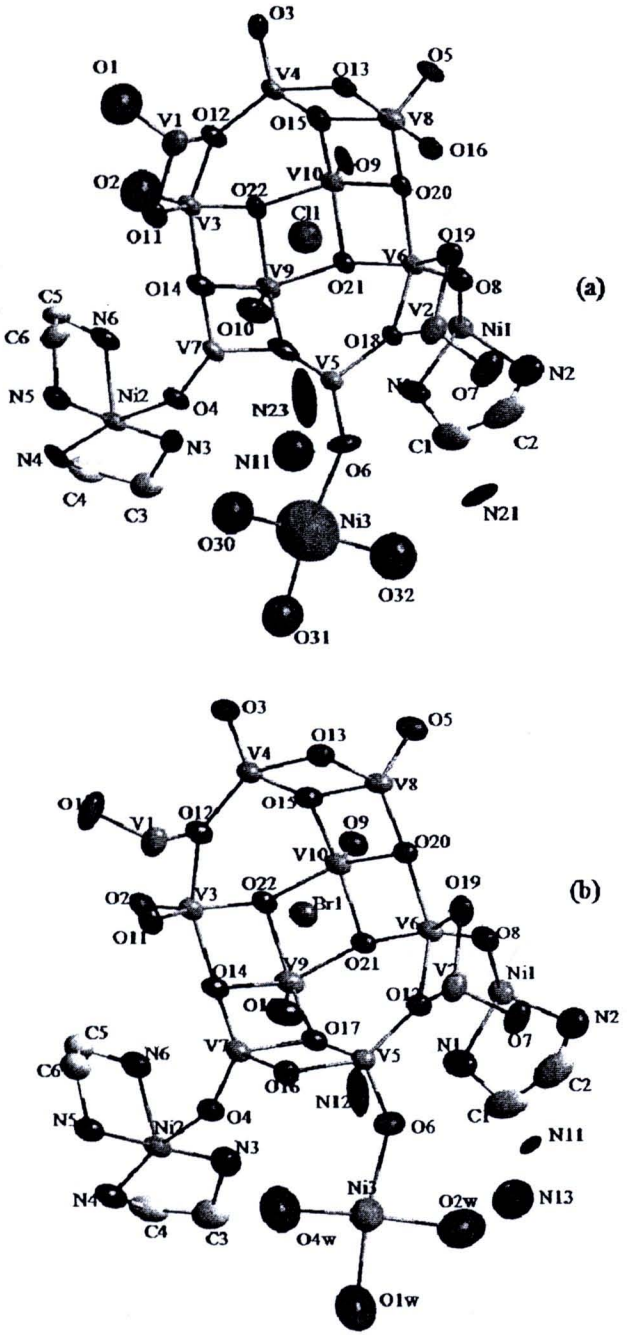

Figure 3.1 Asymmetric units represent local coordination environments of (a) Ni-POV-Cl and (b) Ni-POV-Br presenting with thermal ellipsoid probability of 70%. For clarity H atoms on H_2O, $C_2H_8N_2$ and NH_4^+ have been omitted.

Table 3.2 Fractional atomic coordinates and isotropic or equivalent isotropic displacement parameters ($Å^2$) of atoms in the asymmetric unit of Ni-POV-Cl.

	Ni-POV-Cl			
Atom	**x**	**y**	**z**	**U_{iso}*/U_{eq}**
Ni1	0.0000	0.5000	0.5000	0.0226 (5)
Ni2	0.01354 (12)	0.79800 (7)	0.40500 (7)	0.0193 (4)
V1	0.0000	0.80405 (14)	0.7500	0.0320 (8)
V2	0.0000	0.47957 (13)	0.2500	0.0277 (8)
V3	−0.09439 (17)	0.75979 (9)	0.63803 (9)	0.0195 (5)
V4	−0.18255 (17)	0.23993 (9)	0.30082 (9)	0.0189 (5)
V5	−0.19531 (17)	0.43288 (9)	0.20898(9)	0.0186 (5)
V6	−0.06030 (17)	0.43211 (9)	0.36472 (9)	0.0183 (5)
V7	−0.28301 (16)	0.33225 (9)	0.18833 (9)	0.0197 (5)
V8	−0.26419 (18)	0.34081(10)	0.32636 (10)	0.0257 (5)
V9	−0.13912 (17)	0.65941(9)	0.58964(9)	0.0214 (5)
V10	−0.09062 (17)	0.33173(9)	0.41599 (9)	0.0193 (5)
O1	0.5000	0.6373 (9)	0.2500	0.074 (3)
O2	−0.1335 (13)	0.8015 (6)	0.5882 (7)	0.074 (3)
O3	−0.2596 (7)	0.1972 (4)	0.3233 (4)	0.024 (2)
O4	−0.0981 (7)	0.8303 (4)	0.3410 (4)	0.024 (2)
O5	0.1242 (7)	0.8447 (4)	0.3604 (4)	0.024 (2)
O6	0.2806(8)	0.4748 (4)	0.3112 (5)	0.034 (3)
O7	0.0000	0.5385 (6)	0.2500	0.042 (4)
O8	−0.0828 (7)	0.4740 (4)	0.4178 (4)	0.025 (2)
O9	0.1271 (7)	0.6699 (4)	0.5121 (4)	0.024 (2)
O10	−0.1990 (8)	0.6571 (4)	0.5217 (4)	0.035(3)
O11	−0.1357 (8)	0.7812 (4)	0.7198 (4)	0.029 (2)
O12	−0.0418 (7)	0.2218 (4)	0.3289 (4)	0.025 (2)
O13	−0.2703 (7)	0.2893 (4)	0.2608 (4)	0.022 (2)
O14	−0.2043 (7)	0.7103 (4)	0.6374 (4)	0.026 (2)
O15	−0.1797 (7)	0.2886 (4)	0.3684 (4)	0.025 (2)
O16	−0.2729 (7)	0.3835 (4)	0.2531 (3)	0.0212 (19)
O17	0.2092 (7)	0.3829 (4)	0.3557 (3)	0.025 (2)

Table 3.2 Fractional atomic coordinates and isotropic or equivalent isotropic displacement parameters ($Å^2$) of atoms in the asymmetric unit of Ni-POV-Cl (continued).

	Ni-POV-Cl			
Atom	**x**	**y**	**z**	**U_{iso}*/U_{eq}**
O18	0.0654 (7)	0.4534 (3)	0.3267(4)	0.0186 (18)
O19	−0.1268 (8)	0.4533 (4)	0.2867 (4)	0.028 (2)
O20	−0.1679 (7)	0.3830 (4)	0.3709 (4)	0.0212 (19)
O21	0.0180 (7)	0.3819 (3)	0.4106 (4)	0.0196 (19)
O22	−0.0307 (7)	0.7096 (3)	0.5875 (4)	0.0208 (19)
C1	0.1691 (13)	0.5494 (7)	0.4407 (8)	0.046 (5)
C2	0.0714 (14)	0.5753 (6)	0.4142 (6)	0.046 (5)
C3	0.0906 (12)	0.8550 (6)	0.5119 (7)	0.036 (4)
C4	0.1341 (11)	0.8042 (6)	0.5266 (6)	0.033 (4)
C5	−0.0859 (11)	0.7018 (6)	0.4040 (6)	0.031 (3)
C6	−0.0612 (12)	0.7111 (6)	0.3363 (5)	0.028 (3)
N1	0.1434(9)	0.4995 (5)	0.4549 (5)	0.033 (3)
N2	−0.0118 (11)	0.5697 (5)	0.4598 (5)	0.037 (3)
N3	−0.0099 (9)	0.8502 (4)	0.4744 (5)	0.024 (2)
N4	0.1379 (8)	0.7756 (5)	0.4667 (5)	0.024 (3)
N5	0.0316 (9)	0.7442 (5)	0.3374 (5)	0.031 (3)
N6	−0.0978 (9)	0.7490 (5)	0.4380 (5)	0.027 (3)
Cl1	0.0000	0.3393 (3)	0.2500	0.0464 (15)
Ni3	0.4509 (9)	0.4932 (5)	0.2914 (5)	0.144 (4)
O31	0.6075 (11)	0.5192 (6)	0.2855(7)	0.074 (3)
O30	0.5000	0.4291 (7)	0.2500	0.074 (3)
O32	0.401 (3)	0.5682 (14)	0.3307 (16)	0.090 (10)*
N11	0.367 (3)	0.4434 (15)	0.4472 (17)	0.071 (10)*
N21	0.203 (2)	0.5987 (11)	0.2702 (12)	0.046 (6)*
N23	0.286 (3)	0.4247 (15)	0.541 (2)	0.094 (17)*

Table 3.3 Fractional atomic coordinates and isotropic or equivalent isotropic displacement parameters ($Å^2$) of atoms in the asymmetric unit of Ni-POV-Br.

	Ni-POV-Br			
Atom	**x**	**y**	**z**	U_{iso}*/U_{eq}
Ni1	0.0000	0.5000	0.5000	0.0241 (2)
Ni2	0.51315 (6)	0.29759 (3)	0.40564 (3)	0.02254 (17)
V1	0.0000	0.19349 (6)	0.2500	0.0323 (4)
V2	0.0000	0.48081 (5)	0.2500	0.0270 (3)
V3	0.09388 (8)	0.23900 (4)	0.36109 (4)	0.0214 (2)
V4	−0.18297 (8)	0.23830 (4)	0.29984 (4)	0.02121 (19)
V5	0.19552 (8)	0.43379 (4)	0.29009 (4)	0.02048 (19)
V6	−0.05979 (8)	0.43260 (4)	0.36431 (4)	0.02143 (19)
V7	0.28346 (8)	0.33233 (4)	0.31249 (4)	0.02020 (19)
V8	−0.26388 (9)	0.34062 (4)	0.32610 (4)	0.0229 (2)
V9	0.14054 (9)	0.33967 (4)	0.40893 (4)	0.0242 (2)
V10	−0.09027 (8)	0.33216 (4)	0.41474 (4)	0.0210 (2)
O1	0.0000	0.1333 (3)	0.2500	0.050 (2)
O2	0.1321 (4)	0.19682 (18)	0.4111 (2)	0.0284 (9)
O3	−0.2622 (4)	0.19491 (17)	0.3221 (2)	0.0279 (9)
O4	0.4041 (4)	0.33035 (16)	0.34221 (19)	0.0255 (9)
O5	−0.3756 (4)	0.34346 (18)	0.36089 (19)	0.0284 (9)
O6	0.2809 (4)	0.47645 (19)	0.3080 (2)	0.0347 (11)
O7	0.0000	0.5409 (2)	0.2500	0.0336 (15)
O8	−0.0838 (4)	0.47414 (18)	0.4179 (2)	0.0289 (9)
O9	−0.1275 (4)	0.33103 (17)	0.48699 (19)	0.0260 (9)
O10	0.2019 (4)	0.3415 (2)	0.4773 (2)	0.0377 (12)
O11	0.1358 (4)	0.21774 (17)	0.28055 (19)	0.0271 (9)
O12	−0.0420 (4)	0.21927 (17)	0.32853 (19)	0.0255 (9)
O13	−0.2715 (4)	0.29023 (16)	0.26114 (18)	0.0235 (8)
O14	0.2036 (4)	0.28762 (17)	0.3610 (2)	0.0257 (9)
O15	−0.1800 (4)	0.28860 (16)	0.36682 (19)	0.0246 (9)
O16	0.2725 (4)	0.38296 (16)	0.24682 (18)	0.0235 (8)
O17	0.2095 (3)	0.38405 (16)	0.35579 (17)	0.0218 (8)
O18	0.0663 (4)	0.45437 (16)	0.32608 (18)	0.0225 (8)

Table 3.3 Fractional atomic coordinates and isotropic or equivalent isotropic displacement parameters ($Å^2$) of atoms in the asymmetric unit of Ni-POV-Br (continued).

		Ni-POV-Br		
Atom	**x**	**y**	**z**	U_{iso}*/U_{eq}
O19	−0.1258 (4)	0.45524 (16)	0.28677 (18)	0.0261 (9)
O20	−0.1676 (4)	0.38360 (16)	0.36941 (18)	0.0232 (8)
O21	0.0193 (3)	0.38168 (15)	0.41050 (17)	0.0210 (8)
O22	0.0297 (4)	0.28986 (16)	0.41134 (19)	0.0240 (8)
C1	0.1721 (8)	0.5493 (4)	0.4433 (4)	0.050 (2)
C2	0.0763 (8)	0.5759 (3)	0.4146 (4)	0.048 (2)
C3	0.5933 (7)	0.3555 (3)	0.5116 (3)	0.0389 (17)
C4	0.6346 (6)	0.3039 (3)	0.5259 (3)	0.0346 (15)
C5	0.4140 (6)	0.2000 (3)	0.4054 (3)	0.0323 (14)
C6	0.4401 (6)	0.2099 (3)	0.3370 (3)	0.0310 (13)
N1	0.1438 (5)	0.4977 (2)	0.4577 (3)	0.0357 (13)
N2	−0.0102 (5)	0.5701 (2)	0.4591 (2)	0.0343 (13)
N3	0.4909 (5)	0.3507 (2)	0.4751 (3)	0.0333 (12)
N4	0.6370 (5)	0.2750 (2)	0.4666 (2)	0.0289 (11)
N5	0.5314 (5)	0.2436 (2)	0.3382 (3)	0.0305 (12)
N6	0.4009 (5)	0.2478 (2)	0.4385 (2)	0.0286 (11)
Br1	0.0000	0.33718 (3)	0.2500	0.02834 (19)
Ni3	0.4459 (2)	0.49360 (8)	0.29231 (10)	0.0437 (5)
O2W	0.3977 (16)	0.5689 (7)	0.3358 (12)	0.094 (2)
O4W	0.5000	0.4282 (5)	0.2500	0.094 (2)
O1W	0.3938 (8)	0.5194 (4)	0.2075 (5)	0.094 (2)
N11	0.2002 (9)	0.5965 (3)	0.2743 (6)	0.027 (2)*
N12	0.2817 (14)	0.4223 (5)	0.5438 (7)	0.058 (5)*
N13	0.7106 (19)	0.6117 (7)	0.3404 (15)	0.109 (10)*

Dimension of the $\{V_{18}O_{42}Cl\}$ cluster, measured from V7 to V7′ (-x, y, 0.5-z), V1 to V2 and V10 to V10′ (-x, y, 0.5-z), respectively, is 7.5459(4) Å × 7.6339(6) Å × 7.5113(5) Å, compared to 7.5671(4) Å × 7.7333(6) Å × 7.4579(5) Å for the

$\{V_{18}O_{42}Br\}$ cluster, measured from V7 to V7′ (-x, y, 0.5-z), V1 to V2 and V10 to V10′ (-x, y, 0.5-z) (Figure 3.3).

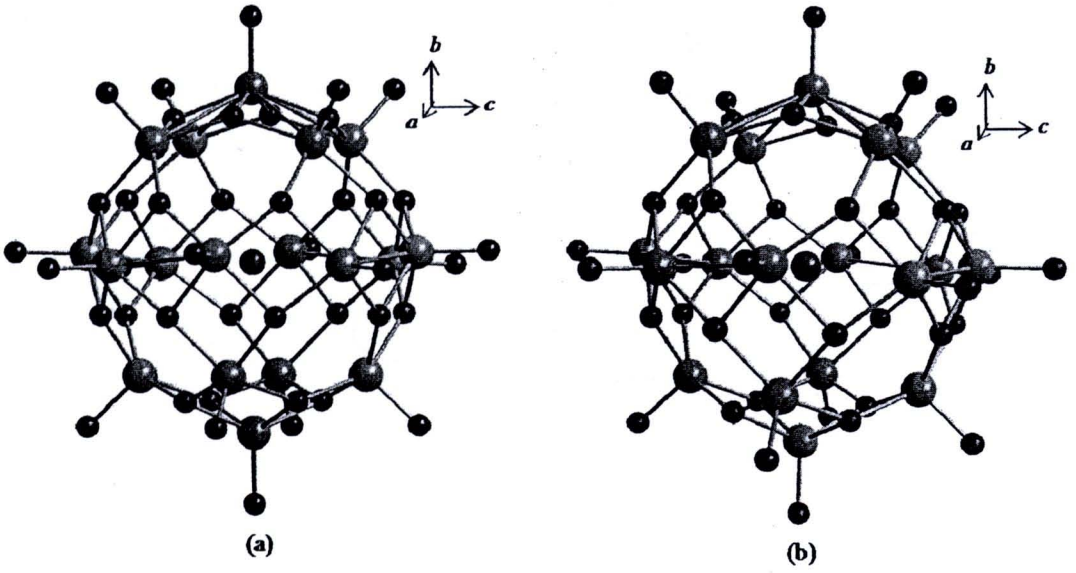

Figure 3.2 Ball and stick representation of (a) $\{V_{18}O_{42}Cl\}$ and (b) $\{V_{18}O_{42}Br\}$ clusters.

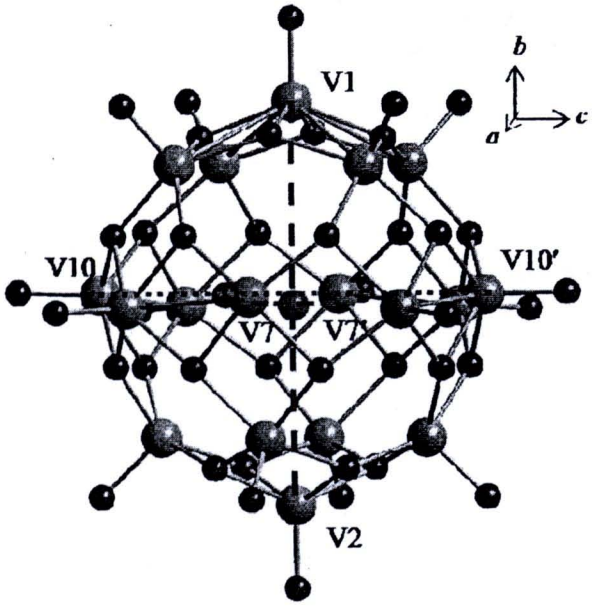

Figure 3.3 Ball and stick representation of determination of dimensionalities in compound clusters.

The curvature of the cluster shell may be estimated also from the distances between the centroids, which can be generated for every four-membered ring using MERCURY 1.4.2 [67] programs. Two distinct curvature angles can be extracted for each cluster (Figure 3.4); 135.31° (*a-b-c*) and 134.57°(*d-a'-b'*) for $\{V_{18}O_{42}Cl\}$ and 135.20° (*a-b-c*) and 134.90°(*d-a'-b'*) for $\{V_{18}O_{42}Br\}$, indicating a close proximity. The influence of a slight difference in ionic radii between Cl^- and Br^- therefore is reflected more in bond lengths and cluster dimension than the cluster shape. This may attribute to the fact that there is enough room for Cl^- (1.81 Å) and Br^- (1.96 Å) to accommodate inside the cluster.

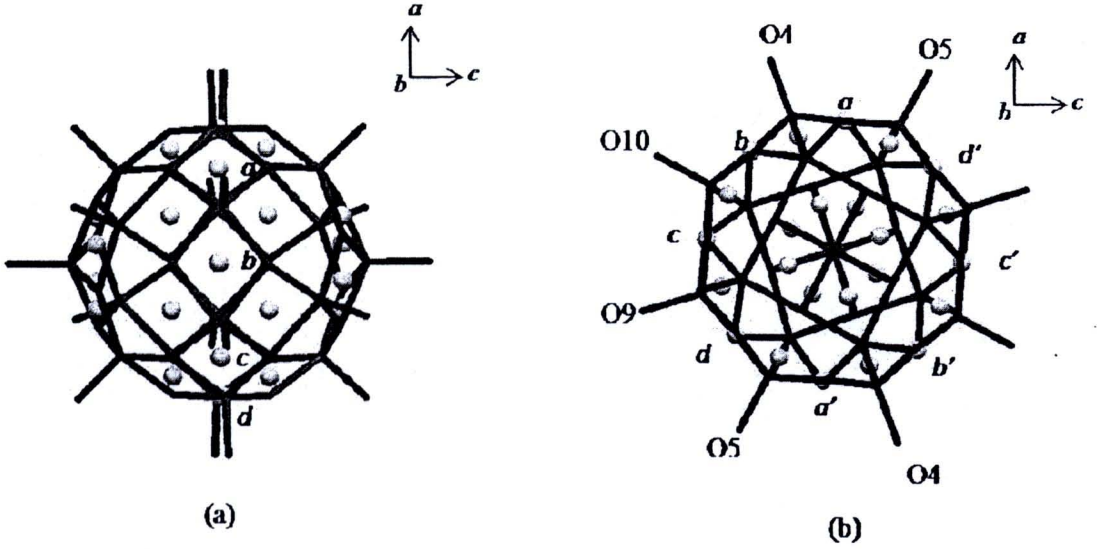

Figure 3.4 Representation of (a) centroid atoms within four-member ring in cluster shells and (b) investigation of angle curve of clusters and labeled atoms relevant to angle curve.

The $\{V_{18}O_{42}\}$ clusters are periodically linked into one-dimensional chain by three nickel complexes between every two adjacent clusters, two of which are *cis*-$[Ni(C_2H_8N_2)_2O_2]^{2+}$and the other is a disordered *cis*-$[Ni(H_2O)_4O_2]^{2+}$, along *a* axis as illustrate in Figure 3.5. The one-dimensional chains of $[V_{18}O_{42}X][Ni(C_2H_8N_2)_2]_2[Ni(H_2O)_4]$ are then connected by *trans*-$[Ni(C_2H_8N_2)_2O_2]^{2+}$ along *c* axis to produce a two-dimensional undulated layer of $[V_{18}O_{42}X][Ni(C_2H_8N_2)_2]_3[Ni(H_2O)_4]$ (Figure 3.6). The undulating angle and a repeating distance and of neighboring clusters on a 1D-chain can be determined as presented in (Figure 3.7). The undulating angles of 101.551(0)° (Cl-Cl′-Cl″) and 100.819(0)° (Br-Br′-Br″) can be measured for Ni-POV-Cl and Ni-POV-Br, respectively. A repeating distance of 21.1968(13) Å is interestingly equal in both two compounds. These layers are stacked along *b* axis, with NH_4^+ cations located in the interlayer gallery (Figure 3.8), acting as a charge compensating unit.

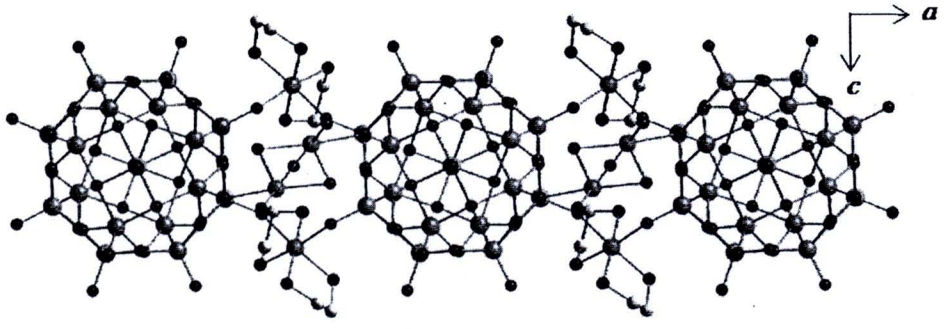

Figure 3.5 The ball and stick representation of the connection of the $[V_{18}O_{42}X]$ cluster in Ni-POV-Cl and Ni-POV-Br forming 1D-chain through Ni groups along *a* axis.

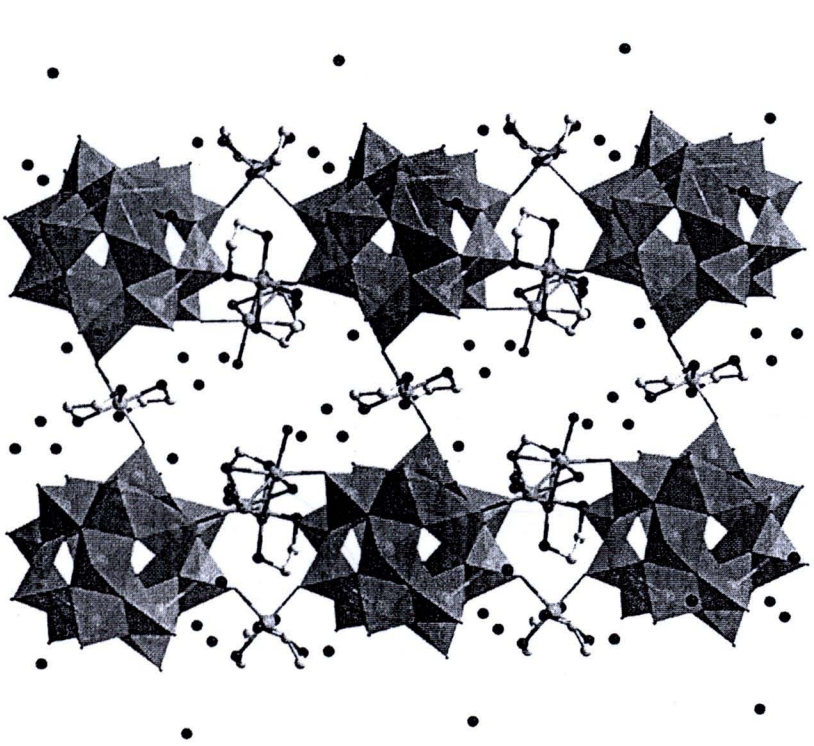

Figure 3.6 The polyhedral representation of the connection of the 1D-chain in Ni-POV-Cl and Ni-POV-Br producing 2D-layer through *trans*-Ni bridging groups along *c* axis. H atoms on H_2O, $C_2H_8N_2$ and NH_4^+ have been omitted for clarity.

The nickel complexes are connected to the $\{V_{18}O_{42}X\}$ clusters *via* the μ_2-O of the clusters, and therefore three types of O atoms can be classified; μ_3-O_b, μ_2-O_b and vanadyl O_t. A slight but meaningful difference in bond lengths involving with V=O_t and V-(μ_2- O) bonds as summarized in Table 3.4, is consistent with the slightly larger size of Br^- (1.96 Å) in Ni-POV-Br in comparison to Cl^- (1.81 Å) in Ni-POV-Cl [68]. The bond lengths of V-O_b bonds are however distributed in a similar range, which may attribute to the limitation of the curvature geometry the V-O_b bonds involved, and the less density of electron cloud in these bonds that have to be shared between any two V atoms they bridge.

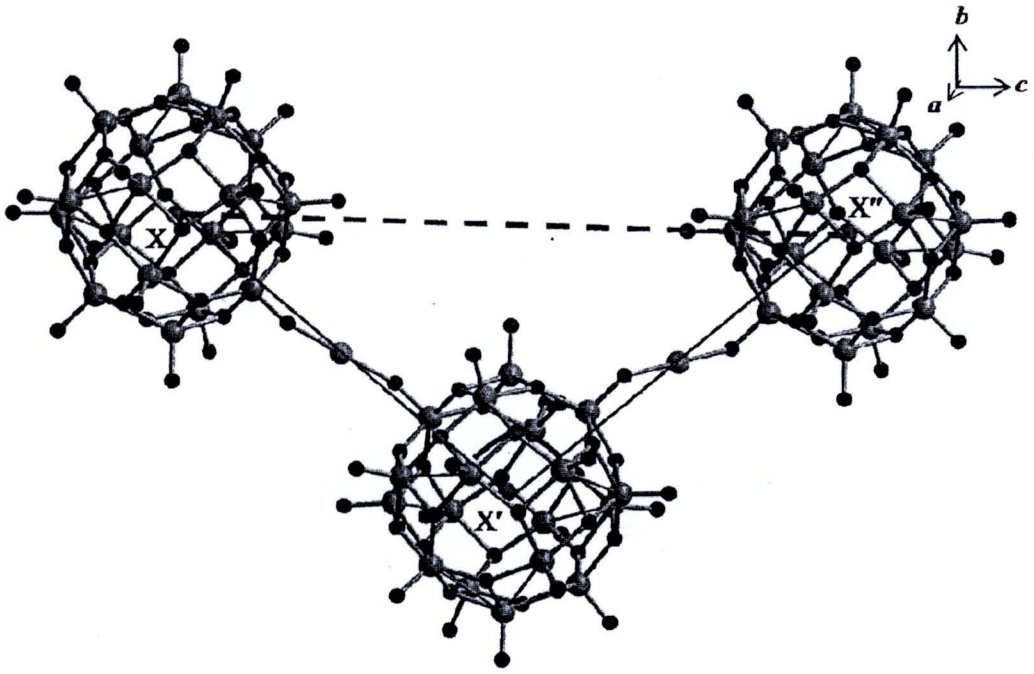

Figure 3.7 The ball and stick representation of the investigation of distance and undulating plane angle in 1D-chain of Ni-POV-Cl and Ni-POV-Br, H_2O, $C_2H_8N_2$ and NH_4^+ have been omitted for clarity.

For every cluster, there are eight nickel complexes; four *cis*-$[Ni(C_2H_8N_2)_2O_2]^{2+}$, two *cis*-$[Ni(H_2O)_4O_2]^{2+}$ and two *trans*-$[Ni(C_2H_8N_2)_2O_2]^{2+}$, decorated on the surface of the cluster, which are generated from three crystallographically distinct nickel atoms. A distorted octahedral geometry of either $\{NiN_4O_2\}_O$ or $\{NiO_6\}_O$ are adopted by every nickel with the involving bond lengths that are equivalent to those of similar structures [3, 8, 20-27]; Ni-(μ_2-O) 2.0813-2.2826 Å, Ni-O(H_2) 2.0098.3201 Å and Ni-N(en) 2.0585-2.1018 Å. The coordination of $\{NiN_4O_2\}_O$ is filled with four N atoms of the chelating en molecules and two *trans*-μ_2-O atoms, when the coordination of the $\{NiO_6\}_O$ motif is completed by four O atoms of the aqua ligand and also two *trans*-μ_2-O atoms. Regarding the locations of

the μ_2-O atoms where the nickel complexes are anchored to each cluster, the μ_2-O atoms position only along *a* and *c* axis with the specific bond angle about 135° (V-μ_2-O-Ni) that can provide more space for the orientation of ethylenediamine ligands.

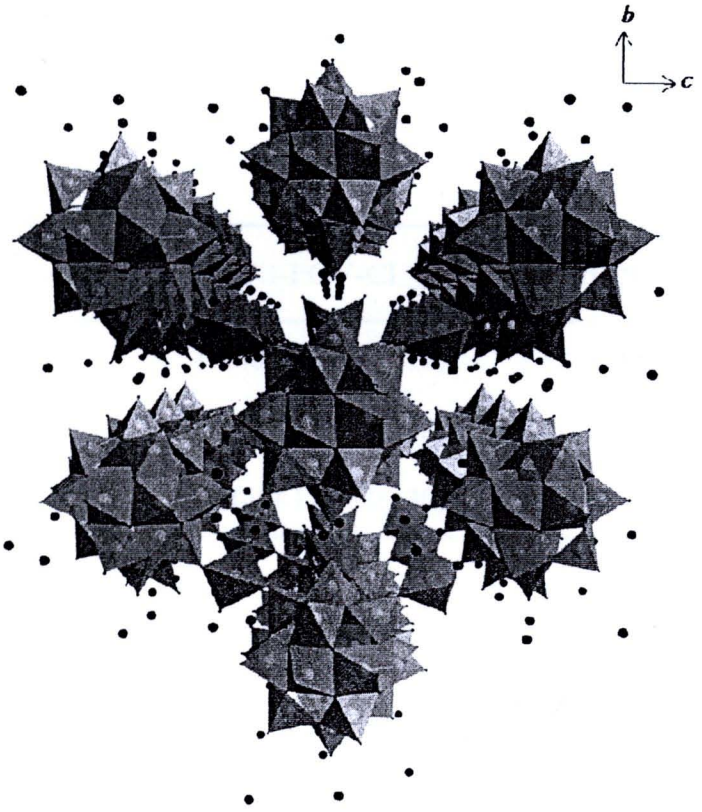

Figure 3.8 The polyhedral representation of the stacking of undulating layers along *b* axis with NH_4^+ cations located in the interlayer gallery of Ni-POV-Cl and Ni-POV-Br.

According to definitions and classification of hydrogen bonding interactions proposed by Steiner [69] as summarized in Table 3.5, the presence of possible interactions in the structures of Ni-POV-Cl and Ni-POV-Br has been analyzed using DIAMOND 3.1 [62] program. As listed in Table 3.6 and 3.7 and depicted in Figure 3.9 to Figure 3.11, most of the possible hydrogen bonding interactions in the

structures is although of moderate or weak types, a cumulative number of these interactions play important role in transfix the orientation of each structural motif including also the intercalated NH_4^+cations in such a way to maximize the attractive forces that important to the stabilization of layer stacking.

Table 3.4 Summarized vanadium-oxygen bond length in clusters for Ni-POV-Cl and Ni-POV-Br

V-O bond	Ni-POV-Cl	Ni-POV-Br
V-(μ_3- O_b)	1.8801-1.9623(212)	1.8876-1.9607(179)
V=O_t	1.5579-1.6153(188)	1.6126-1.6274(78)
V-(μ_2- O_b)	1.6090-1.6281(130)	1.6140-1.6359(98)

Table 3.5 The criterion used to identify the strength types of hydrogen bond.

	Strong	Moderate	Weak
A–H····B interaction	mostly covalent	mostly electrostatic	electrostatic
Bond lengths	A–H ≈ H····B	A–H < H····B	A–H << H····B
H····B (Å)	~1.2-1.5	~1.5-2.2	2.2-3.2
A····B (Å)	2.2-2.5	2.5-3.2	3.2-4.0
Bond angle (°)	175-180	130-180	90-150
Bond energy (kcal mol^{-1})	14-40	4-15	<4
Relative IR $\nu_s$vibration shift (cm^{-1})	25%	10-25%	<10%
H^1 chemical shift downfield (ppm)	14-22	<14	-

Table 3.6 List of hydrogen bonds in the structure of Ni-POV-Cl.

D-H····A (Å)	d(H····A) (Å)	d(D····A) (Å)	D-H····A angle (°)
Interlayer hydrogen bond			
Moderate hydrogen bonds			
N(4)–H(4C)····O9	2.0995(105)	3.0085(169)	168.716(864)
Weak hydrogen bonds			
O(32)–H(32A)····O(1)	2.4177(122)	2.8606(401)	108.114(2190)
O(31)–H(31A)····O(1)	2.7655(193)	3.5299(269)	134.356(920)
C(4)–H(4A)····O(3)	2.8098(84)	3.4905(152)	126.543(774)
C(4)–H(4A)····O(15)	3.1699(101)	3.3781(176)	93.518(863)
C(4)–H(4B)····O(2)	2.9692(166)	3.7081(217)	132.239(855)
C(4)–H(4B)····O(12)	2.5463(86)	3.4056(159)	145.045(785)
C(4)–H(4B)····O(15)	2.7994(97)	3.3781(176)	117.902(847)
C(5)–H(5A)····O(10)	2.6561(89)	3.1778(167)	113.164(806)
C(5)–H(5B)····C(2)	3.1535(164)	3.9484(228)	138.269(930)
C(5)–H(5B)····N(2)	3.1166(173)	3.8481(205)	131.755(916)
C(4)–H(4A)····N(4)	3.0081(121)	3.6067(187)	120.062(863)
N(4)–H(4D)····C(4)	3.1384(151)	3.6067(187)	113.587(726)
Intralayer hydrogen bond			
Moderate hydrogen bonds			
N(5)–H(5D)····O(3)	0.9204(111)	2.9705(140)	151.397(705)

Table 3.6 List of hydrogen bonds in the structure of Ni-POV-Cl (continued).

D-H····A (Å)	d(H····A) (Å)	d(D····A) (Å)	D-H····A angle (°)
Intralayer hydrogen bond			
Weak hydrogen bonds			
O(31)–H(31A)····O(32)	2.5352(339)	2.7945(379)	94.578(1210)
O(31)–H(31B)····O(19)	3.0007(103)	3.8210(178)	141.124(862)
O(31)–H(31B)····O(30)	3.0260(118)	2.8602(222)	70.945(839)
O(30)– H(30A)····O(4)	3.2493(98)	3.5517(173)	99.636(165)
(30)–H(30A)····O(16)	2.3731(91)	3.1398(118)	133.719(217)
O(30)–H(30A)····O(31)	3.0406(160)	2.8602(222)	76.146(289)
O(30)–H(30A)····O(5)	2.6526(95)	3.5780(153)	155.688(201)
O(30)–H(30B)····O(4)	3.3006(96)	3.5780(153)	96.310(163)
O(30)–H(30B)····O(16)	2.3731(91)	3.1398(118)	133.719(217)
O(30)–H(30B)····O(31)	3.0406(160)	2.8620(222)	70.146(289)
O(30)–H(30B)····O(5)	2.6526(95)	3.5780(153)	155.688(201)
N(5)–H(5D)····N(4)	2.9068(112)	3.1146(151)	94.352(717)
C(1)–H(1B)····O(9)	3.0073(105)	3.6294(12)	121.935(1074)
C(1)–H(1B)····O(8)	2.8866(91)	3.3041(193)	106.317(997)
C(1)–H(1A)····O(6)	3.0168(107)	3.7369(207)	130.559(1013
C(2)–H(2A)····O(18)	3.0544(81)	3.7668(174)	129.985(863)
C(2)–H(2B)····O(8)	3.0406(101)	3.3636(196)	100.449(974)
C(2)–H(2B)····O(9)	2.7583(93)	3.3393(179)	118.083(85)
C(4)–H(4A)····O(9)	2.5941(91)	3.2621(168)	124.851(837)

Table 3.6 List of hydrogen bonds in the structure of Ni-POV-Cl (continued).

D-H····A (Å)	d(H····A) (Å)	d(D····A) (Å)	D-H····A angle (°)
Intralayer hydrogen bond			
Weak hydrogen bonds			
C(3)–H(3B)····O(9)	3.1763(92)	3.7154(179)	115.834(901)
C(3)–H(3B)····O(5)	2.8151(87)	3.2722(173)	108.912(879)
C(5)–H(5A)····O(2)	2.7794(166)	3.5857(217)	139.093(883)
C(6)–H(6B)····O(4)	2.8545(107)	3.2447(194)	104.385(951)
C(6)–H(6B)····O(14)	3.0121(96)	3.7232(182)	129.785(918)
C(6)–H(6B)····O(11)	3.1429(100)	3.9893(179)	144.488(849)
N(5)–H(5D)····O(13)	3.0980(95)	3.2989(149)	94.428(740)
N(1)–H(1D)····O(8)	2.8067(89)	3.0276(145)	94.911(738)
N(1)–H(1D)····O(18)	2.2341(84)	3.1058(138)	157.845(721)
N(1)–H(1D)····O(21)	3.0687(83)	3.6474(153)	122.559(800)
N(1)–H(1D)····O(6)	2.9912(107)	3.6484(155)	129.704(707)
N(1)–H(1D)····O(17)	3.1149(100)	3.8926(159)	143.413(759)
N(2)–H(2D)····O(8)	2.8467(94)	3.0438(144)	93.488(757)
N(2)–H(2D)····O(9)	2.6747(100)	3.3828(166)	134.561(829)
N(2)–H(2D)····O(10)	3.1079(104)	3.6386(170)	118.658(826)
N(2)–H(2D)····O(21)	2.2106(85)	3.0448(140)	150.731(728)
N(6)–H(6D)····O(2)	3.0898(163)	3.6980(201)	125.239(781)
N(6)–H(6D)····O(14)	2.2801(88)	3.1164(144)	150.875(750)
N(6)–H(6D)····O(10)	3.0038(104)	3.7450(162)	138.726(778)
N(6)–H(6D)····O(4)	2.8090(97)	3.0025(156)	93.078(754)

Table 3.6 List of hydrogen bonds in the structure of Ni-POV-Cl (continued).

D-H····A (Å)	d(H····A) (Å)	d(D····A) (Å)	D-H····A angle (°)
Intralayer hydrogen bond			
Weak hydrogen bonds			
N(4)–H(4D)····O(9)	2.6527(93)	3.3418(143)	132.260(686)
N(4)–H(4D)····O(5)	2.6809(94)	2.9203(151)	95.745(741)
N(4)–H(4D)····O(15)	2.3436(89)	3.2163(139)	158.171(680)
N(5)–H(5D)····O(13)	3.0980(95)	3.2989(149)	94.428(740)
N(5)–H(5C)····O(13)	2.7392(92)	3.2989(149)	120.083(732)
N(5)–H(5C)····O(5)	2.8558(100)	2.9819(167)	88.770(787)
N(5)–H(5C)····O(3)	3.0954(94)	2.9734(151)	73.818(758)
N(5)–H(5C)····O(4)	2.7644(99)	2.8480(164)	85.723(770)
N(3)–H(3C)····O(4)	2.8907(90)	3.0370(135)	90.240(695)
N(3)–H(3D)····O(10)	3.0492(101)	3.7166(154)	130.840(737)
N(5)–H(5C)····C(6)	3.1587(119)	3.8247(150)	130.768(688)
N(3)–H(3D)····N(6)	2.8016(128)	3.0298(169)	95.397(710)

Hydrogen bond of ammonium cations			
D····A (Å)	**d(D····A) (Å)**	**D····A (Å)**	**d(D····A) (Å)**
Moderate hydrogen bonds		Weak hydrogen bonds	
N(23)····O(10)	2.7604(400)	N(11)····O(10)	3.5324(410)
N(21)····O(3)	2.8890(307	N(11)····O(4)	3.8269(403)
N(21)····O(7)	3.0834(279)	N(11)····O(17)	3.1757(384)
N(21)····O(32)	2.8800(447)	N(23)····N(3)	3.6437(406)

Table 3.6 List of hydrogen bonds in the structure of Ni-POV-Cl (continued).

D····A (Å)	d(D····A) (Å)	D····A (Å)	d(D····A) (Å)
Hydrogen bond of ammonium cations			
Weak hydrogen bonds			
N(23)····N(2)	3.4680(407)	N(23)····O(8)	3.8807(407)
N(11)····C(1)	3.8024(433)	N(23)····O(2)	3.5640(429)
N(11)····C(3)	3.9081(413)	N(21)····O(11)	3.9895(303)
N(21)····C(1)	3.8893(313)	N(21)····O(1)	3.9503(267)
N(21)····C(2)	3.6063(299)	N(21)····O(31)	3.4833(313)
N(23)····N(1)	3.2490(397)	N(21)····O(6)	3.5825(310)

Table 3.7 List of hydrogen bonds in the structure of Ni-POV-Br.

D-H····A (Å)	d(H····A) (Å)	d(D····A) (Å)	D-H····A angle (°)
Interlayer hydrogen bond			
Moderate hydrogen bonds			
N(4)–H(4C)····O9	2.1144(1)	3.0219(2)	168.676(6)
Weak hydrogen bonds			
O(1W)–H(1w1)····O(1)	2.7216(1)	3.4500(2)	130.720(6)
C(4)–H(4A)····O(3)	2.8549(2)	3.5389(2)	126.891(3)
C(4)–H(4A)····O(15)	3.1748(2)	3.4018(2)	94.678(4)
C(4)–H(4B)····O(2)	2.9649(2)	3.7089(2)	132.756(4)
C(4)–H(4B)····O(12)	2.5598(2)	3.4141(2)	144.454(3)
C(4)–H(4B)····O(15)	2.8287(1)	3.4018(2)	117.551(4)
C(5)–H(5A)····O(10)	2.6423(2)	3.1585(2)	112.643(3)

Table 3.7 List of hydrogen bonds in the structure of Ni-POV-Br(continued).

D-H····A (Å)	d(H····A) (Å)	d(D····A) (Å)	D-H····A angle (°)
Interlayer hydrogen bond			
Weak hydrogen bonds			
C(5)–H(5B)····C(2)	3.1332(2)	3.9250(2)	137.984(5)
C(4)–H(4A)····N(4)	2.9722(1)	3.5959(2)	121.897(5)
C(5)–H(5B)····N(2)	3.0607(2)	3.7887(2)	131.382(5)
N(4)–H(4D)····C(4)	3.1188(1)	3.5952(2)	114.204(5)
Intralayer hydrogen bond			
Moderate hydrogen bonds			
N(5)–H(5D)····O(3)	2.1262(1)	2.9699(1)	151.965(6)
Weak hydrogen bonds			
O(4W)–H(4w1)····O(4)	3.3135(2)	3.5322(2)	94.515(4)
O(4W)–H(4w2)····O(5)	2.6530(1)	3.5880(2)	157.550(4)
O(2W)–H(12)····C(1)	3.0758(2)	3.7894(2)	130.513(3)
N(5)–H(5D)····N(4)	2.8821(1)	3.0935(2)	94.504(3)
C(1)–H(1B)····O(9)	2.9794(2)	3.5987(2)	121.631(4)
C(1)–H(1B)····O(8)	2.8347(1)	3.2616(2)	106.807(3)
C(1)–H(1A)····O(6)	3.0765(1)	3.7933(2)	130.354(3)
C(2)–H(2A)····O(9)	2.7188(1)	3.3026(2)	118.096(4)
C(2)–H(2B)····O(18)	3.0521(2)	3.7720(2)	130.597(4)
C(2)–H(2B)····O(8)	3.1183(2)	3.4195(2)	99.217(5)
C(4)–H(4A)····O(9)	2.5956(1)	3.2591(2)	124.421(5)

Table 3.7 List of hydrogen bonds in the structure of Ni-POV-Br (continued).

D-H····A[a] (Å)	d(H····A) (Å)	d(D····A) (Å)	D-H····A angle (°)
Intralayer hydrogen bond			
Weak hydrogen bonds			
C(3)–H(3B)····O(9)	3.1319(2)	3.6769(2)	116.129(4)
C(3)–H(3B)····O(5)	2.7884(2)	3.2525(2)	109.284(3)
C(5)–H(5A)····O(2)	2.7971(1)	3.5995(2)	138.571(5)
C(6)–H(6B)····O(11)	3.1514(2)	4.0037(2)	145.102(4)
C(6)–H(6B)····O(14)	3.0047(1)	3.7218(2)	130.240(5)
C(6)–H(6B)····O(4)	2.9011(2)	3.2761(2)	103.452(6)
N(1)–H(1D)····O(17)	3.0681(2)	3.8586(2)	145.091(4)
N(1)–H(1D)····O(6)	3.0777(2)	3.7381(2)	130.202(3)
N(1)–H(1D)····O(21)	3.0354(2)	3.6218(2)	123.189(5)
N(1)–H(1D)····O(8)	2.8317(2)	3.0468(2)	94.606(4)
N(2)–H(2D)····O(9)	2.6540(1)	3.3567(2)	133.756(5)
N(2)–H(2D)····O(8)	2.8688(1)	3.0562(2)	92.862(3)
N(2)–H(2D)····O(10)	3.1582(1)	3.7086(2)	120.317(4)
N(2)–H(2C)····O(8)	2.7159(2)	2.8693(2)	90.117(5)
N(4)–H(4D)····O(5)	2.6586(1)	2.8990(1)	95.743(4)
N(4)–H(4D)····O(9)	2.6864(1)	3.3654(2)	131.305(5)
N(3)–H(3C)····O(4)	2.8800(1)	3.0258(2)	90.157(3)
N(3)–H(3D)····O(10)	3.0386(2)	3.6916(2)	129.389(5)
N(5)–H(5D)····O(13)	3.1093(1)	3.3074(2)	94.258(4)
N(5)–H(5C)····O(13)	2.7476(1)	3.3074(2)	120.201(4)

Table 3.7 List of hydrogen bonds in the structure of Ni-POV-Br (continued).

D-H····A (Å)	d(H····A) (Å)	d(D····A) (Å)	D-H····A angle (°)
Intralayer hydrogen bond			
Weak hydrogen bonds			
N(6)–H(6D)····O(4)	2.8314(1)	3.0187(1)	92.742(4)
N(6)–H(6D)····O(10)	2.9694(1)	3.6975(2)	137.184(5)
N(6)–H(6D)····O(2)	3.0940(1)	3.7066(2)	125.676(5)
N(5)–H(5C)····C(6)	3.1915(2)	3.8559(2)	130.784(3)
N(3)–H(3D)····N(6)	2.8631(2)	3.0831(2)	95.023(5)
O(4W)–H(4w2)····O(1W)	3.0907(2)	2.9246(2)	71.125(5)
O(4W)–H(4w2)····O(4)	3.2029(1)	3.5322(2)	101.251(4)
O(4W)–H(4w1)····O(5)	2.6530(1)	3.5880(2)	157.550(4)
O(4W)–H(4w1)····O(16)	2.3945(1)	3.1397(2)	131.536(5)
O(4W)–H(4w1)····O(1W)	3.0907(2)	2.9246(2)	71.125(5)
O(1W)–H(1w2)····O(19)	3.0666(1)	3.8315(2)	135.031(5)
O(1W)–H(1w1)····O(2W)	2.8159(2)	3.0235(2)	92.387(3)
O(4W)–H(4w2)····O(16)	2.3945(1)	3.1397(2)	131.536(5)
O(4W)–H(4w2)····O(1W)	3.0907(2)	2.9246(2)	71.125(5)
O(1W)–H(1w2)····O(4W)	3.0805(1)	2.9246(2)	71.684(4)
Hydrogen bond of ammonium cations			
D····A (Å)	**d(D····A) (Å)**	**D····A (Å)**	**d(D····A) (Å)**
Moderate hydrogen bonds			
N(13)····O(2)	2.9386(1)	N(11)····O(2W)	2.8672(2)

Table 3.7 List of hydrogen bonds in the structure of Ni-POV-Br (continued).

D-H····A (Å)	d(H····A) (Å)	d(D····A) (Å)	D-H····A angle (°)
Hydrogen bond of ammonium catio			
Moderate hydrogen bonds			
N(13)····O(1W)	2.9636(2)	N(11)····O(7)	2.9824(1)
N(11)····O(3)	2.8621(2)	N(12)····O(10)	2.7501(1)
Weak hydrogen bonds			
N(13)····C(5)	3.7488(2)	N(12)····N(1)	3.2058(2)
N(13)····O(11)	3.2145(2)	N(12)····N(2)	3.4331(2)
N(13)····O(1)	3.2301(2)	N(12)····N(3)	3.6734(2)
N(12)····O(2)	3.4961(2)	N(11)····C(2)	3.4662(2)
N(12)····O(8)	3.8550(2)	N(11)····C(1)	3.8219(2)
N(11)····O(6)	3.4536(2)	N(13)····C(6)	3.9492(2)
N(11)····O(1W)	3.5718(2)		

Figure 3.12 shows the powder X-ray diffraction patterns collected from the ground crystals of Ni-POV-Cl and Ni-POV-Br. The nearly identical patterns of Ni-POV-Cl and Ni-POV-Br exhibit the presence of only a few intense diffraction peaks in a low 2θ region is the characteristic for two-dimensional layered structure where preferred orientation is inherent. The interlayered *d*-spacing can be calculated for the (010) and (020) planes [70], giving identical value of 13.4893 Å for both Ni-POV-Cl and Ni-POV-Br. This is consistent with the interlayer spacing of 13.4575 Å, measured from X^- atom to X^- atom in the [010] direction.

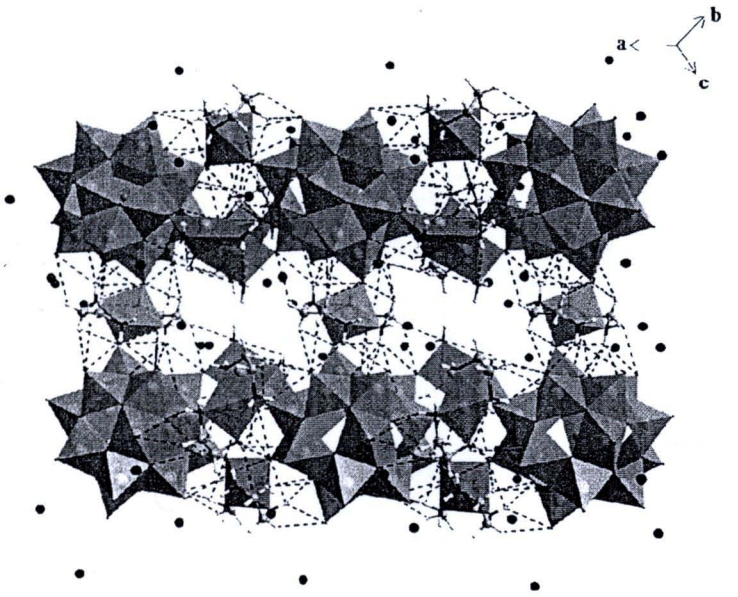

Figure 3.9 Illustration of hydrogen bonding interaction in intralayer of Ni-POV-Cl.

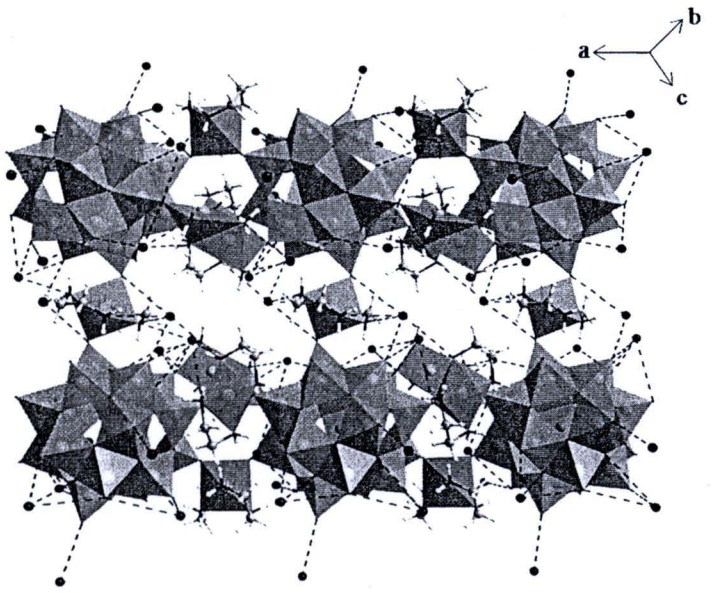

Figure 3.10 Illustration of hydrogen bonding interaction of ammonium ions in Ni-POV-Cl compounds.

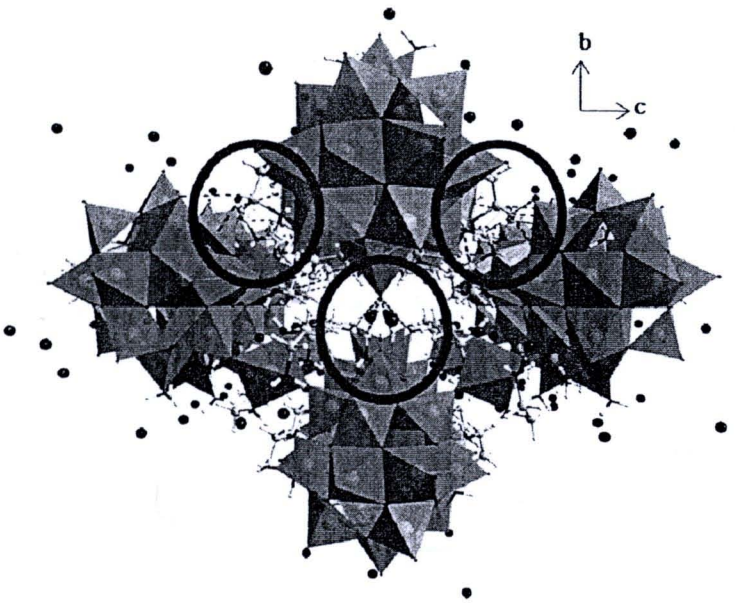

Figure 3.11 Illustration of hydrogen bonding interaction in interlayer of Ni-POV-Cl.

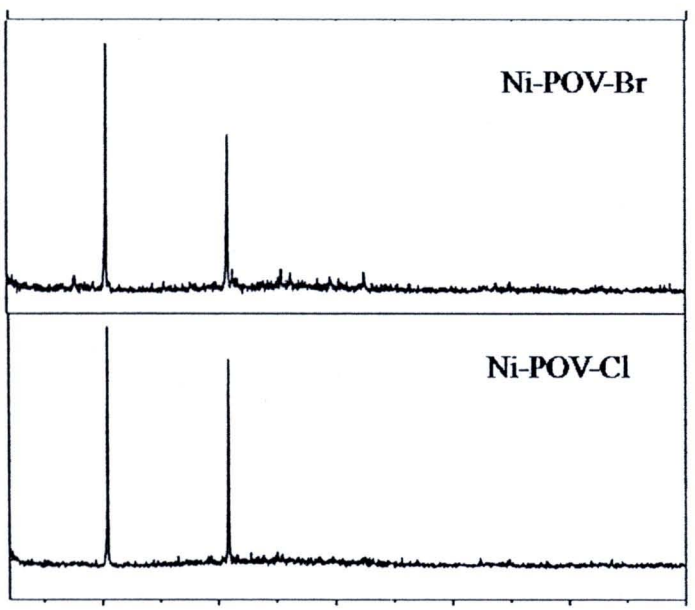

Figure 3.12 Comparison of the powder X-ray diffraction patterns of Ni-POV-Cl and Ni-POV-Br.

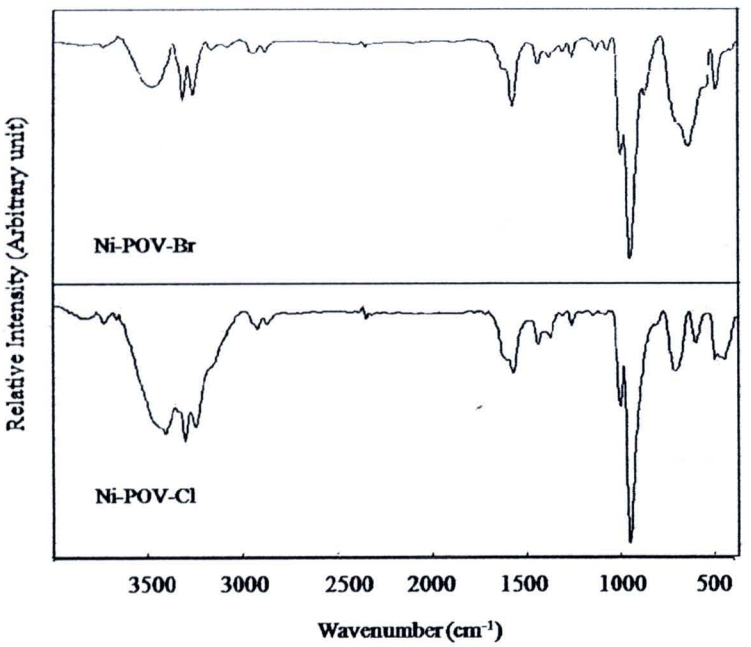

Figure 3.13 FT-IR spectra confirming the presence of the lattice ammonium cations, ethylenediamines and an absent of lattice water within the structures of Ni-POV-Cl and Ni-POV-Br.

The FT-IR spectra collected on the selected crystals of Ni-POV-Cl and Ni-POV-Br are shown in Figure 3.13; with the band assignments listed in Table 3.8. The presence of the absorption bands at 1454 cm^{-1} which is characteristic to the NH_4^+, and the absence of the characteristic deformation band of free H_2O at 1630 cm^{-1} eliminate doubtfulness on the assignment of the NH_4^+ instead of water molecules in the interlayered space.

Although, the energy dispersive X-ray microanalysis results taken on surfaces of various crystals of Ni-POV-Cl and Ni-POV-Br are not in accordance to the

crystallographic formulas, as summarized in Table 3.9 and 3.10, respectively, they provide primary elemental components in the compounds.

Table 3.8 Spectral assignments for the FT-IR spectra of Ni-POV-Cl, Ni-POV-Br and Ni-POV-I.

Ni-POV-Cl		**Ni-POV-Br**	
Wave number (cm^{-1})	**Assignments**	**Wave number (cm^{-1})**	**Assignments**
3312vs	ν(N-H)	3311vs	ν(N-H)
2934s, br	ν_{as}(C-H), CH_2	1588s	δ_{as}(N-H)
1560s	δ_{as}(N-H)	1455m	δ_s(N-H), NH_4^+
1454s	δ_s(N-H), NH_4^+	1278m	δ_s(N-H)
1278s	δ_s(N-H)	1149m	ν(C-N)
1024vs	ν(C-N)	1094s	ν(C-N)
971vs	ν_{as}(V-O_t)	1018s	ν(C-N)
707s	ν_{as}(V-(μ_3-O))	972vs	ν_{as}(V-O_t)
519s	ν_s(V-O_b-V)	660s	ν_{as}(V-O_b-V)
		518s	ν_s(V-O_b-V)

vs = very sharp, s = sharp, m = medium, w = weak, br = broad, ν_s = symmetric stretching, ν_{as} = asymmetric stretching, δ_s = symmetric bending, δ_{as} = asymmetric bending

Table 3.9 The element component from EDS data for Ni-POV-Cl.

Elements	Weight%	Experimental (Atomic %)
C	11.75	22.65
N	14.24	23.54
O	20.64	29.88
V	40.29	18.32
Ni	11.33	4.47
Cl	1.75	1.15

Table 3.10 The element component from EDS data for Ni-POV-Br.

Elements	Weight%	Experimental (Atomic %)
C	7.96	19.01
N	7.94	16.25
O	15.79	28.31
V	50.33	28.33
Ni	12.73	6.22
Br	5.24	1.88

3.2 Structural description of Ni-POV-I

Figure 3.14 and Figure 3.15 show the powder X-ray diffraction pattern and the FR-IR spectrum of the selected Ni-POV-I crystals. It is plain that the diffraction pattern is different from those of Ni-POV-Cl and Ni-POV-Br but partially agreement with the single crystal structures. The powder X-ray diffraction pattern shows rather noisy background with more diffraction peaks compared to the other two structures, with less pronounced preferred-orientation effect. On the other hand, FT-IR spectrum appears to be mostly similar to those of Ni-POV-Cl and Ni-POV-Br and assignment spectrum was listed in Table 3.11.

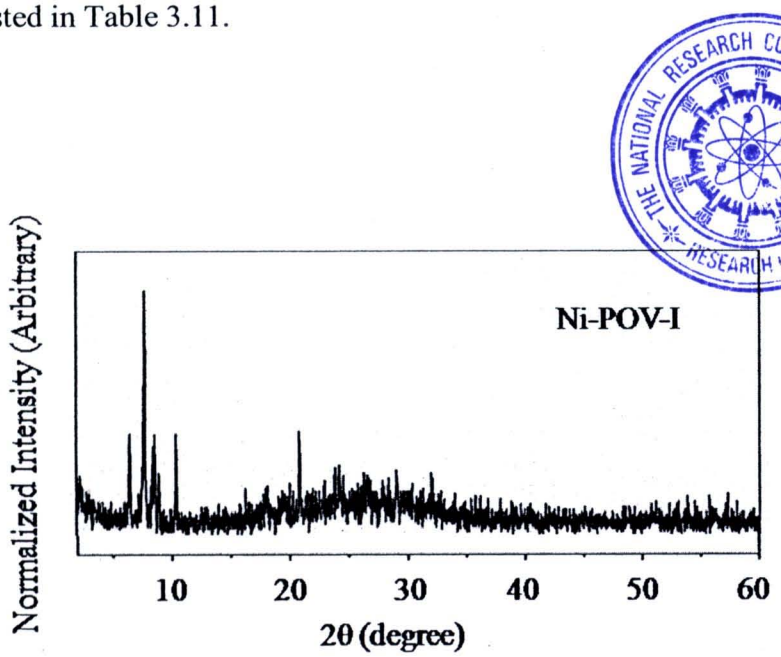

Figure 3.14 Powder X-ray diffraction patterns of Ni-POV-I presenting some impurities in bulk sample.

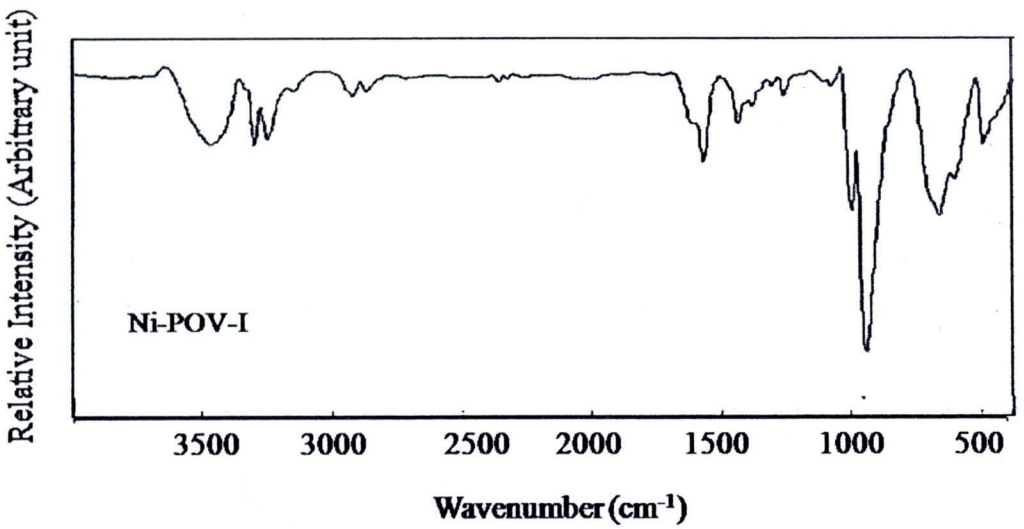

Figure 3.15 FT-IR spectra confirming the presence of the lattice ammonium cations, ethylenediamines and an absent of lattice water within the structures of Ni-POV-I.

Table 3.11 Spectral assignments for the FT-IR spectrum of Ni-POV-I.

Ni-POV-I			
Wave number (cm^{-1})	**Assignments**	**Wave number (cm^{-1})**	**Assignments**
3311vs	ν(N-H)	1122w	ν(C-N)
2933w, br	ν_{as}(C-H), CH_2	1024vs	ν(C-N)
1590s	δ_{as}(N-H)	965vs	$\nu_{as}(V\text{-}O_t)$
1455s	δ_s(N-H), NH_4^+	685s	$\nu_{as}(V\text{-}O_b\text{-}V)$
1278s	δ_s(N-H)	519s	$\nu_s(V\text{-}O_b\text{-}V)$

vs = very sharp, s = sharp, m = medium, w = weak, br = broad, ν_s = symmetric stretching, ν_{as} = asymmetric stretching, δ_s = symmetric bending, δ_{as} = asymmetric bending

The semi-quantitative analysis on the surface of the Ni-POV-I crystals give the elementary compositional elements that composed of C, N, O, V, Ni and especially I^- as detailed in Table 3.12.

Table 3.12 The element component from EDS data for Ni-POV-I.

Elements	Experimental (Atomic %)	Experimental ratio
C	21.71	13.9
N	15.97	10.2
O	31.08	19.9
V	24.07	15.4
Ni	5.60	3.6
I	1.56	1.0

Numbers of crystals of Ni-POV-I have been chosen for the single crystal X-ray diffraction experiments, but the collected data contain difficulties in possibly both twinning and disorder feature in the structure. It has been attempted to solve the structure in the same monocline *C2/c* (No. 15) space group as the Ni-POV-Cl and Ni-POV-Br cases, but it was not successful. The sub-group *C2/m* (No. 12) space group has been also endeavored solving the structure, but disorder of atoms still exists. Until now the primary crystal structure of Ni-POV-I might be $[V_{18}O_{42}I]$ $[Ni(C_2H_8N_2)_3](NH_4)_3$, but the other structural descriptions are not complete.

3.3 Determination of Valences for Vanadium

The bond valence sum (BVS) calculation is a common method which is used in determining atom valences in crystal structures, and has been attempted with the Ni-POV-X structures. The BVS results which are dependent on different R_0 values are listed in Table 3.13. It is apparent that the obtained values are distributed between 4 and 5, from which the exact values of valences cannot be concluded although the mixed valence of V^{IV}/V^{V} can be assumed. The uncertainty in the calculation of exact number of V^{IV} and V^{V} can be brought about by the average bond lengths due to the high nuclearity and therefore high electron density of the clusters.

The manganometric titration and the back titration with sulfur dioxide gas have been attempted with the Ni-POV-Br sample, for a determination of numbers of existing V^{IV} and the total number of vanadium in the form of V^{IV}, respectively. The manganometric titration results suggest 16.90 V^{IV} and the back titration gave the total number of 18.40 for V^{IV}, meaning that there should be $1.5V^{V}$ and $16.90V^{V}$. These numbers can be rounded to $2V^{V}$ and $16V^{IV}$ with a certain degree of bias to make up to 18V in total, which results in a negative $\{V^{IV}_{16}V^{V}_{2}O_{42}Br\}^{-11}$ cluster.

Due to the inconsistency of the experimental results as described, computational chemistry has been applied. The DMol^3 calculations based on charge density distribution using density functional theory (DFT) have been performed for the structures of Ni-POV-Cl, Ni-POV-Br and Ni-POV-I [53].Various methods of BLYP [53], PBE [57] and PW91 [53] with double numerical plus a polarization *d*-function have been tried in the generalized gradient approximation to obtain the Mulliken population analysis using the Materials Studio program [71]. In order to

interpret the Mulliken charges to atomic valences, the assumptions of 18:0 and 16:2 for the V^{IV}:V^{V} have been proposed in the calculations.

Table 3.13 Bond valence sum calculation of vanadium atoms in cluster with various R_0 parameters.

R_0 / Vanadium atoms	1.784 [a]	1.803 [b]	1.788 [c]
Ni-POV-Cl			
V1	4.5707	4.8116	4.6377
V2	4.3204	4.5481	4.3547
V3	4.4132	4.6143	4.4107
V4	4.3735	4.6040	4.4034
V5	4.3601	4.5898	4.3818
V6	4.3530	4.5824	4.3624
V7	4.3664	4.5965	4.3893
V8	4.1916	4.4124	4.1851
V9	4.5192	4.7574	4.5664
V10	4.4033	4.6353	4.4262
Ni-POV-Br			
V1	4.3575	4.5871	4.3729
V2	4.2621	4.4866	4.2683
V3	4.4262	4.6277	4.4194
V4	4.1483	4.3668	4.1370
V5	4.3038	4.5305	4.3164
V6	4.2717	4.4968	4.2693
V7	4.2007	4.4220	4.1914
V8	4.2666	4.4914	4.2623
V9	4.3617	4.5916	4.3817
V10	4.3288	4.5568	4.3371

[a,b] Using b = 0.37, R_0 = 1.784 and 1.803 for V^{IV}-O and V^{V}-O bond, respectively from I.D. Brown, *Accumulated Table of Bond Valence Parameters*

[c] Using b = 0.32, R_0 = 1.788 from I.D. Brown, *Chemical Reviews*, **109** (2009) 6870.

It is evident that different methods of calculations provide the same results as illustrated in Figure 3.16, Table 3.14 to 3.16, indicating the presence of both $V^{IV}$and V^{V}in the atomic ratio of 16:2 for everycompound. When the other atomic ratios for V^{IV}:V^{V} are attempted in the calculation of the Mulliken charge, they result in the unmatched number of V^{IV} that has been previously assessed with the number of the V^{IV} in the range of the calculated atomic Mulliken charge. For example, in the case of Ni-POV-I, when the atomic ratio of 14:4 was attempted for V^{IV}:V^{V}, only $8V^{IV}$ are in a range of the calculated atomic Mulliken charge of V^{IV}. It, therefore, can be concluded that the vanadium valences found in the structures of Ni-POV-Cl, Ni-POV-Br and Ni-POV-I are the same, which is $16V^{IV}$:$2V^{V}$ and therefore the negative clusters of $\{V^{IV}_{16}V^{V}_{2}O_{42}X\}^{-11}$.

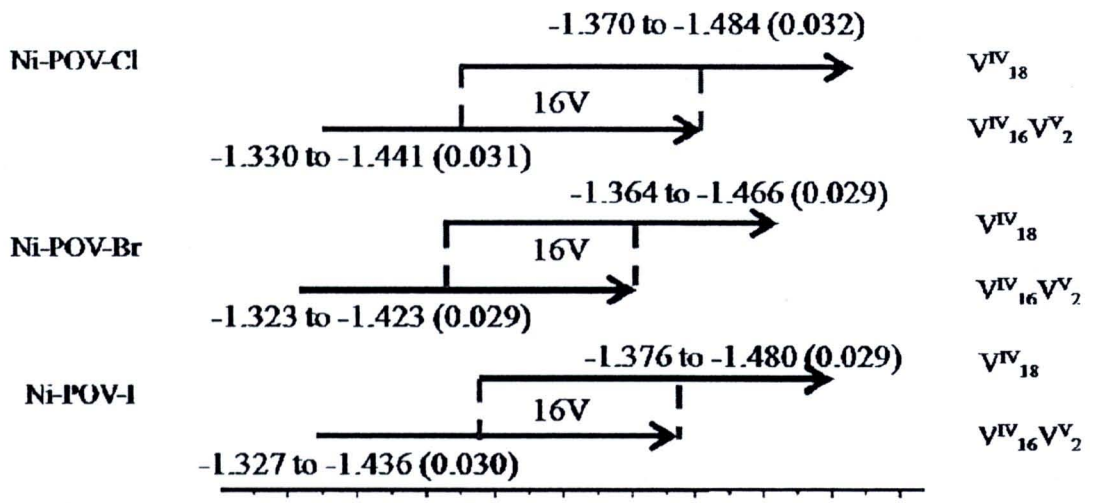

Figure 3.16 An example of an overlap range of the $16V^{IV}$ from BLYP method calculated atomic Mulliken charge of $16V^{IV}$:$2V^{V}$ appearing in the range of atomic Mulliken charge of V^{IV}.

Table 3.14 Mulliken net atomic charges (a.u.) resulted from various methods for Ni-POV-Cl.

	Cluster type	Atom[a]									
		V1	V2	V3	V4	V5	V6	V7	V8	V9	V10
BLYP	$V^{IV}_{18}O_{42}$	-1.370	-1.390	-1.481	-1.482	-1.484	-1.479	-1.445	-1.445	-1.454	-1.450
	$V^{V}_{18}O_{42}$	-1.009	-1.009	-1.097	-1.099	-1.106	-1.104	-1.064	-1.057	-1.070	-1.071
	$V^{IV}_{16}V^{V}_{2}O_{42}$	-1.330	-1.347	-1.438	-1.439	-1.441	-1.437	-1.403	-1.402	-1.411	-1.407
PBE	$V^{IV}_{18}O_{42}$	-1.464	-1.481	-1.592	-1.593	-1.596	-1.591	-1.547	-1.545	-1.558	-1.553
	$V^{V}_{18}O_{42}$	-1.093	-1.090	-1.197	-1.199	-1.206	-1.205	-1.155	-1.146	-1.163	-1.164
	$V^{IV}_{16}V^{V}_{2}O_{42}$	-1.423	-1.437	-1.547	-1.549	-1.552	-1.548	-1.504	-1.500	-1.514	-1.510
PW91	$V^{IV}_{18}O_{42}$	-1.444	-1.460	-1.574	-1.575	-1.577	-1.572	-1.529	-1.527	-1.540	-1.535
	$V^{V}_{18}O_{42}$	-1.075	-1.073	-1.181	-1.183	-1.190	-1.190	-1.139	-1.131	-1.148	-1.148
	$V^{IV}_{16}V^{V}_{2}O_{42}$	-1.403	-1.417	-1.530	-1.531	-1.534	-1.53	-1.485	-1.482	-1.496	-1.492

[a] The calculated vanadium atoms performed only the atoms in asymmetric unit.

Table 3.15 Mulliken net atomic charges (a.u.) resulted from various methods for Ni-POV-Br.

	Cluster type	Atom[a]									
		V1	V2	V3	V4	V5	V6	V7	V8	V9	V10
BLYP	$V^{IV}_{18}O_{42}$	-1.364	-1.383	-1.464	-1.463	-1.466	-1.456	-1.424	-1.435	-1.425	-1.426
	$V^{V}_{18}O_{42}$	-0.999	-1.001	-1.082	-1.079	-1.086	-1.083	-1.044	-1.046	-1.050	-1.053
	$V^{IV}_{16}V^{V}_{2}O_{42}$	-1.323	-1.341	-1.421	-1.420	-1.423	-1.414	-1.382	-1.392	-1.383	-1.384
PBE	$V^{IV}_{18}O_{42}$	-1.456	-1.475	-1.578	-1.573	-1.579	-1.569	-1.525	-1.537	-1.528	-1.530
	$V^{V}_{18}O_{42}$	-1.082	-1.082	-1.185	-1.178	-1.188	-1.185	-1.135	-1.138	-1.143	-1.147
	$V^{IV}_{16}V^{V}_{2}O_{42}$	-1.414	-1.431	-1.534	-1.529	-1.535	-1.526	-1.482	-1.493	-1.485	-1.487
PW91	$V^{IV}_{18}O_{42}$	-1.436	-1.455	-1.559	-1.554	-1.559	-1.549	-1.506	-1.519	-1.509	-1.511
	$V^{V}_{18}O_{42}$	-1.064	-1.065	-1.169	-1.162	-1.172	-1.168	-1.118	-1.122	-1.127	-1.130
	$V^{IV}_{16}V^{V}_{2}O_{42}$	-1.394	-1.411	-1.515	-1.510	-1.516	-1.507	-1.463	-1.475	-1.467	-1.468

[a] The calculated vanadium atoms performed only the atoms in asymmetric unit.

Table 3.16 Mulliken net atomic charges (a.u.) resulted from various methods for Ni-POV-I.

	Cluster type	Atom[a]									
		V1	**V2**	**V3**	**V4**	**V5**	**V6**	**V7**	**V8**	**V9**	**V10**
BLYP	$V^{IV}_{18}O_{42}$	-1.376	-1.394	-1.476	-1.480	-1.476	-1.469	-1.434	-1.440	-1.446	-1.446
	$V^{V}_{18}O_{42}$	-1.007	-1.013	-1.088	-1.091	-1.095	-1.093	-1.054	-1.054	-1.066	-1.066
	$V^{IV}_{16}V^{V}_{2}O_{42}$	-1.327	-1.351	-1.433	-1.436	-1.433	-1.427	-1.391	-1.398	-1.403	-1.403
PBE	$V^{IV}_{18}O_{42}$	-1.459	-1.486	-1.588	-1.592	-1.588	-1.581	-1.534	-1.543	-1.552	-1.550
	$V^{V}_{18}O_{42}$	-1.091	-1.095	-1.189	-1.192	-1.197	-1.194	-1.144	-1.145	-1.161	-1.160
	$V^{IV}_{16}V^{V}_{2}O_{42}$	-1.419	-1.443	-1.543	-1.547	-1.544	-1.538	-1.491	-1.498	-1.508	-1.506
PW91	$V^{IV}_{18}O_{42}$	-1.439	-1.466	-1.569	-1.573	-1.569	-1.562	-1.515	-1.524	-1.533	-1.531
	$V^{V}_{18}O_{42}$	-1.073	-1.077	-1.173	-1.176	-1.181	-1.178	-1.128	-1.129	-1.145	-1.143
	$V^{IV}_{16}V^{V}_{2}O_{42}$	-1.398	-1.423	-1.525	-1.529	-1.526	-1.519	-1.472	-1.480	-1.490	-1.488

[a] The calculated vanadium atoms performed only the atoms in asymmetric unit.

The conclusion on the mixed valence and negative $\{V^{IV}_{16}V^{V}_{2}O_{42}X\}^{-11}$ cluster is in good agreement with the statistical analysis of the reported structures involving with $\{V_{18}O_{42}\}$ cluster proposed by Muller *et.al* in 1997 [8]. Characteristic differences of the basic $\{V^{IV}_{18}O_{42}\}$, $\{V^{IV}_{16}V^{V}_{2}O_{42}\}$ and $\{V^{IV}_{10}V^{V}_{8}O_{42}\}$ anions have been proposed as useful tool in defining degree of valence mixing in these anions. For example, the vibrational spectroscopic ν_{as} for the vanadyl V=O_t group should be about 950 cm^{-1} for the $\{V^{IV}_{18}O_{42}\}$, and between 965-970 cm^{-1} for the $\{V^{IV}_{16}V^{V}_{2}O_{42}\}$, when the distances between the cluster V atoms and the encapsulated anion are to be between 3.76 Å and 3.80 Å for the $\{V^{IV}_{18}O_{42}\}$, and between 3.73 Å and 3.75 Å for the $\{V^{IV}_{16}V^{V}_{2}O_{42}\}$. In the case of Ni-POV-Cl, Ni-POV-Br and Ni-POV-I, the data analysis conducted on the single crystal structure well correspond with the proposed values for $\{V^{IV}_{16}V^{V}_{2}O_{42}\}$; ν_{as} (V=O_t) of 971, 972 and 965 $cm^{-1}$for Ni-POV-Cl, Ni-

POV-Br and Ni-POV-I, respectively. Table 3.17 lists the distances measured from the central anion to the cluster V atoms for these structures.

Table 3.17 Characteristic physical data used to determine vanadium valencies for Ni-POV-Cl and Ni-POV-Br.

Characteristic data	Ni-POV-Cl	Ni-POV-Br
r_{av} (V_{18})[a] (Å)		
V1	3.8674(3)	3.8579(3)
V2	3.8659(3)	3.7759(3)
V3	3.6989(2)	3.7297(2)
V4	3.7234(2)	3.7359(2)
V5	3.6709(2)	3.6161(2)
V6	3.6369(2)	3.5954(2)
V7	3.7858(2)	3.7777(2)
V8	3.798(2)	3.8033(2)
V9	3.7376(2)	3.756(2)
V10	3.7314(2)	3.7611(2)
Average r_{av} (V_{18})	3.7516(732)	3.7409(760)

[a] Average distance between the V atoms of the $\{V_{18}O_{42}\}$ shell and its center.

3.4 UV-vis Spectroscopic and Thermogravimetric Analysis

The UV-vis spectra of the synthesized Ni-POV-X have been collected from the solutions prepared from dissolving the selected ground crystals in 1 mmol·dm^{-3} of H_2SO_4 solution, in a range between 200 and 800 nm. Figure 3.17 show the collected spectra with the assignment listed in Table 3.18, revealing similar features of the

single strong and broad absorption band in a region between 200 nm and 300 nm. This can be attributable to the LMCT of $O_t \rightarrow V$ and $(\mu\text{-O}) \rightarrow V$ [72-74]. The broad band without a maxima observed in the spectra of the three compounds may be due to a large number of vanadium atoms present in the structures with closely similar electronic transition energies [75]. The weak broad band is additionally observed at 760 nm, which can be according to the V^{4+} to V^{5+} transitions $d_{xy} \rightarrow d_{xz}, d_{yz}$ for the oxovanadium(IV) chromophore [76].

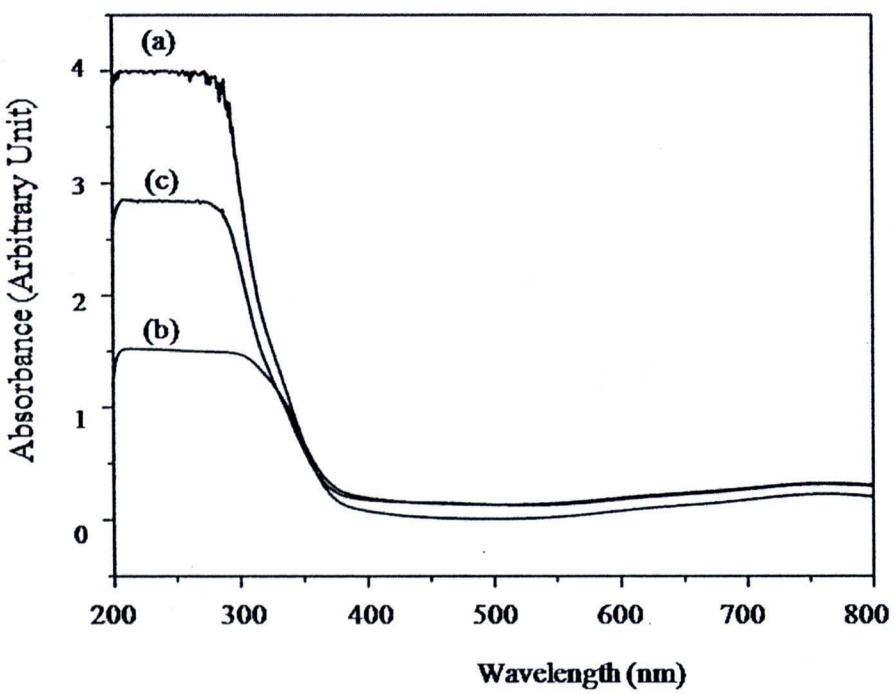

Figure 3.17 Illustration of UV-vis spectra of (a) Ni-POV-Cl, (b) Ni-POV-Br and (c) Ni-POV-I mmol/dm^{-3} of H_2SO_4 solution.

Although the square-pyramidal geometry is adopted by V atoms in the $\{V_{18}O_{42}\}$ cluster, a general orbital splitting energy diagrams as shown in Figure 3.18 (a) and Figure 3.18 (b) cannot be sufficiently used for the interpretation of the

involving electronic transition. For vanadium oxide clusters like Ni-POV-Cl, Ni-POV-Br and Ni-POV-I, the unusual energy diagram as shown in Figure 3.18 (c) is generally adopted because of the curvature exhibited by the cluster structure [77].

Table 3.18 UV-vis absorption data for Ni-POV-Cl, Ni-POV-Br and Ni-POV-I in 1 mmol/dm^{-3} of H_2SO_4 solution.

Compounds	UV-Vis, nm (ε, mol·dm^{-3}·cm^{-1})
Ni-POV-Cl	217(4000), 248(4000),763(227)
Ni-POV-Br	212(1523), 760(324)
Ni-POV-I	216(2860), 268(2846), 760(315)

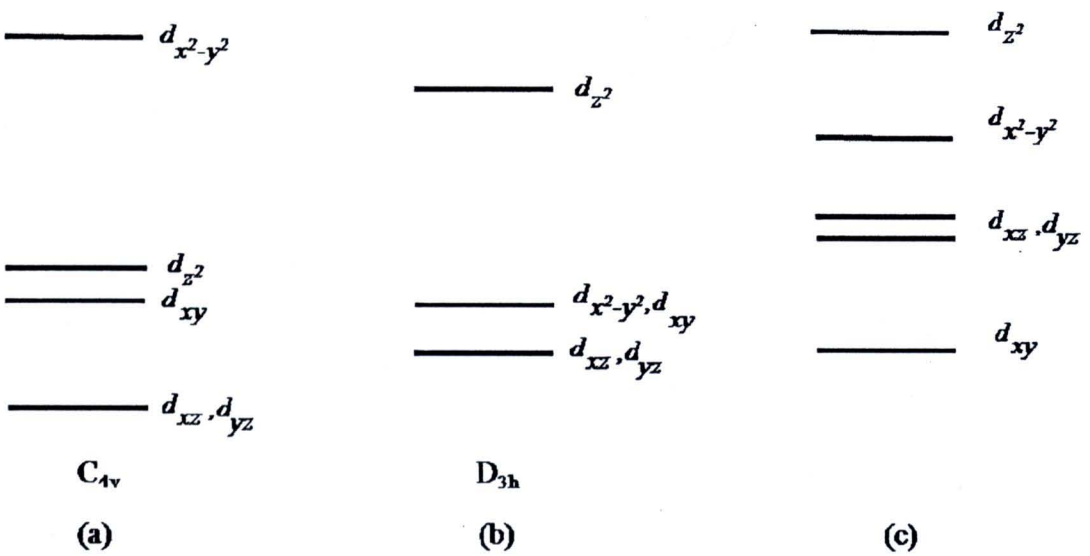

Figure 3.18 Energy levels diagram of *3d* orbitals for five-coordinate complexes in (a) C_{4v}, (b) D_{3h} fields and (c) energy diagram of oxovanadium(IV) complexes [77].

The thermogravimetric curves of Ni-POV-Cl and Ni-POV-Br are shown in Figure 3.19, revealing similar pattern of weight losses for Ni-POV-Cl and Ni-POV-Br. Four weight losses can be observed in the cases of Ni-POV-Cl and Ni-POV-Br, which should be due to the subsequent liberation of the intercatalated NH_4^+, the aqua ligand and the chelating en, as summarized in Table 3.19.

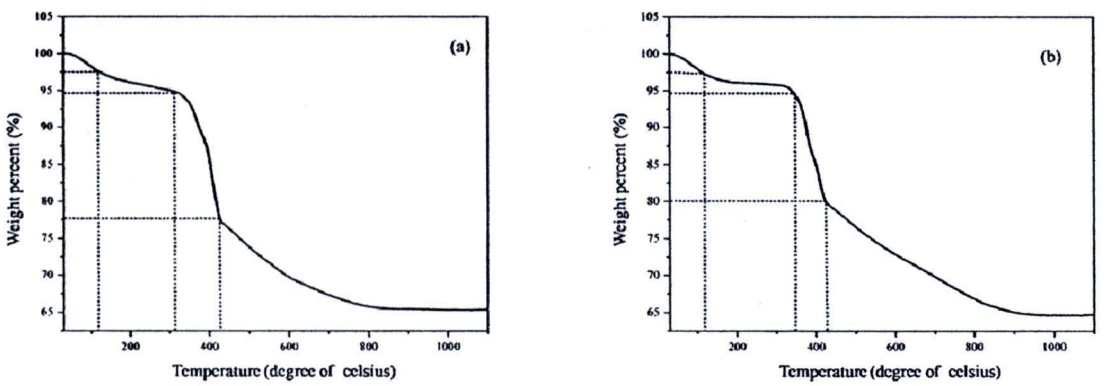

Figure 3.19 TGA curves showing the weight losses observed upon heating the ground crystals of (a) Ni-POV-Cl and (b) Ni-POV-Br.

3.5 Magnetic Properties of Ni-POV-Cl and Ni-POV-Br

The field dependent specific magnetization, M(H), curves obtained from the isothermal VSM measurements of selected crystals of Ni-POV-Cl and Ni-POV-Br are shown in Figure 3.20 and 3.21, respectively, elucidating how the induced magnetization varied with the applied magnetic field. The unusual loops were obtained. For Ni-POV-Cl, it is slightly similar to paramagnetic hysteresis loop but, the unidentified gap at very low and high applied field still cannot explain. The wide range of gap in loop for Ni-POV-Br appearing around -5000 Oe applied field onwards

leads this magnetic results cannot unfold. For resolve this problem, SQUID measurements will have been attempted to study magnetic properties of compounds.

Table 3.19 Weight losses data from thermogravimetric analysis.

Compounds	Molecule losses	Liberation temperature ranges (°C)	Experimental weight losses (%)	Theoretical weight losses (%)
Ni-POV-Cl	ammonia	below 133.00	2.75	2.18
	water ligand	133.00-351.20	4.00	3.07
	ethylendiamine ligand	351.20-426.00	16.00	15.37
Ni-POV-Br	ammonia	below 116.25	2.50	2.14
	water ligand	116.25-348.75	3.00	3.01
	ethylendiamine ligand	348.75-422.50	14.50	15.09

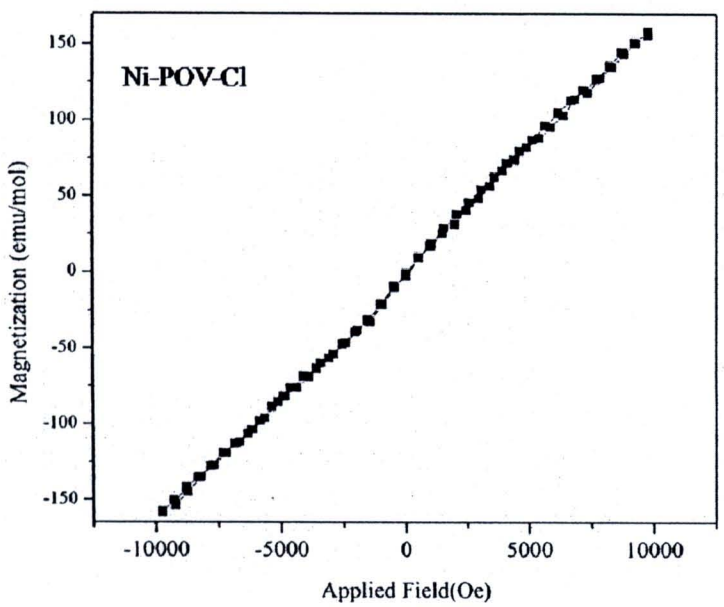

Figure 3.20 Field dependent specific magnetization curves of the selected crystals of Ni-POV-Cl at 298 K.

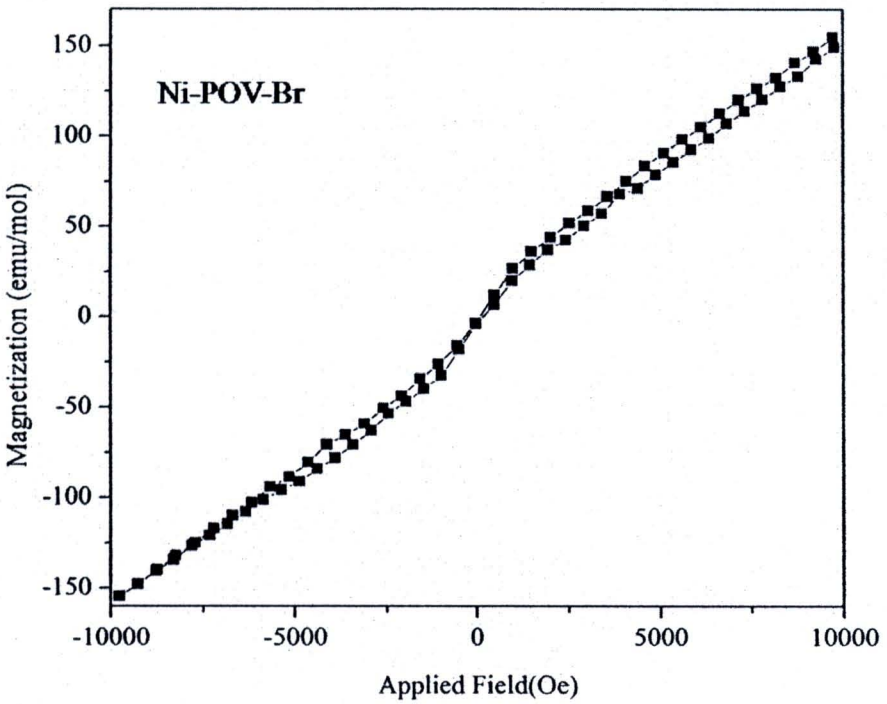

Figure 3.21 Field dependent specific magnetization curves of the selected crystals of Ni-POV-Br at 298 K.